Conducted EMI Issues in a Boost PFC Design

L. Rossetto

University of Padova
Department of Electrical Engineering
Via Gradenigo 6/A - 35131 Padova - ITALY
E-Mail: leopoldo@tania.dei.unipd.it

S. Buso, G.Spiazzi

University of Padova
Department of Electronics and Informatics
Via Gradenigo 6/A - 35131 Padova - ITALY
E-Mail: simone@tania.dei.unipd.it

***Abstract* - The paper presents the results of an experimental activity concerned with the development of a 600W Boost Power Factor Corrector (PFC) complying with the EMC standards for conducted EMI in the 150kHz-30MHz range. In order to accomplish this task, different circuit design and layout solutions are taken into account and their effect on the conducted EMI behavior of the converter is experimentally evaluated. Common-mode and differential-mode switching noise, together with input filters' design and topology and with the PCB layout (in terms of track length and spacing, ground and shielding planes etc.) are the key aspects which have been analyzed. In particular, the paper reports the conducted EMI measurements for different filter capacitor placements and values, for different power switch drive circuits together with several other provisions which have turned out to be decisive in the reduction of the generated EMI.**

I. INTRODUCTION

The employment of Boost Power Factor Correctors (PFC's) in order to comply with the IEC 1000-3-2 low frequency EMC standard [1]-[3] is becoming more and more ordinary in a large variety of industrial applications of SMPS's. This solution, however, increases the conducted interference generation of the power supply in the high frequency range. As a consequence, while the low frequency harmonic content of the current driven from the utility grid is normally well controlled and compliant with the aforementioned IEC standard, the high frequency currents generated by the converter on the grid may be beyond the corresponding standard limits [4]-[7]. To avoid this, it is very important to properly design the EMI filters and the circuit layout so as to minimize the effects of the switching converter on the line pollution. The paper discusses the design of a 600W Boost PFC complying with the EMC standards for conducted EMI in the 150kHz-30MHz range [8]. Different circuit design and layout solutions are taken into account and their effect on the conducted EMI behavior of the converter is experimentally evaluated. Common-mode and differential-mode switching noise, together with input filters' design and topology and with the PCB layout (in terms of track length and spacing, ground and shielding planes etc.) are the key aspects which have been analyzed. In particular, the paper reports the conducted EMI measurements for different filter capacitor placements and values, different power switch drive circuits together with several other provisions, which have turned out to be decisive in reducing the conducted EMI level of the converter [9]. By means of this design example, the paper also shows that the application of the theoretically derivable EMC basic design rules, which in principle should guarantee the limitation of the EMI in a switching power converter, may, in some cases, become partially ineffective because of second order effects (e.g. resonances, component parasitics, connections). The experimental results illustrate these unexpected outcomings and the validity of the adopted provisions which allow to design a fully compliant power supply.

II. BASIC SCHEME OF THE CONVERTER

Fig. 1 shows the basic scheme of the considered Boost PFC. The ratings of the converter are reported in Table I. These represent the typical characteristics of a PFC designed for a large variety of applications (e.g. telecom applications). A conventional and simple design procedure can be adopted to derive the necessary passive components' values, required to guarantee the continuous conduction mode of operation for the converter practically during the whole line period and a suitable output voltage ripple level. Also the selection of the required switch and diode is

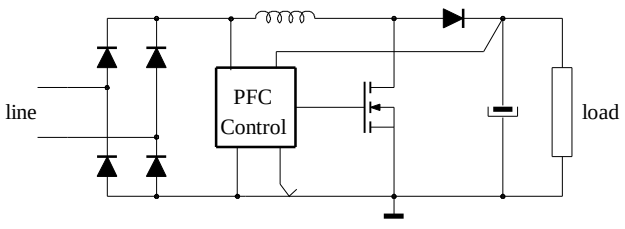

Fig. 1 - Basic scheme of the Boost PFC.

almost straightforward, given the current and voltage stresses, which are easily determined analyzing the converter's typical waveforms. The resulting list of adopted components is reported in Table II.

TABLE I
CONVERTER RATINGS

Input voltage (RMS)	90-260 V
Output power	600 W
Output voltage	380 V
Switching Frequency	70kHz

TABLE II
MAIN CONVERTER COMPONENTS

Output capacitor	680 μF
Inductor	600 μH
Mosfet	IRFP450
Diode	RURP1560
Controller IC	L4981A

III. CONSIDERATIONS ON THE POWER STAGE DESIGN

The considered topology is simple and well known [10]-[13]. However, when it comes to EMI control, it is necessary to adopt particular care in the definition of the layout of the power stage [14]-[18].

Of course, the main sources of EM noise can be easily identified in the power switch and diode. The reduction of the wire lengths for the current return paths and for the high dv/dt circuit branches, together with the reduction of the areas embraced by high di/dt loops, as is shown in Fig. 2, appear to be fundamental provisions. It is therefore fundamental that the area between the power switch and the two high frequency by-pass capacitors, which are used to drain the current pulses generated during the commutations, are made as small as possible. Indeed, if the emitting area is small, the efficiency of the equivalent loop antenna, indicated by the arrow in Fig. 2, is small

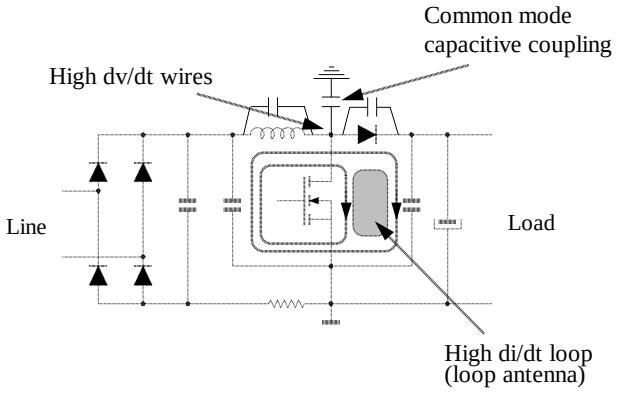

Fig. 2 - Critical points of the circuit for EMI generation.

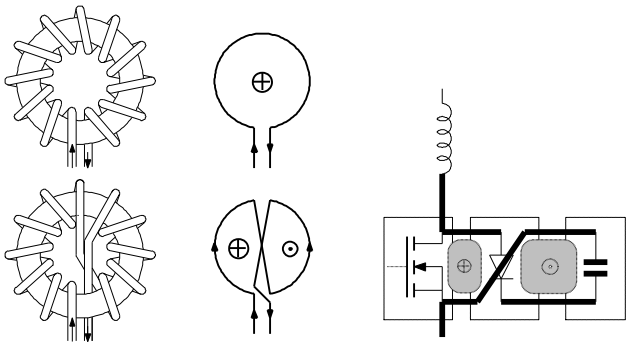

a) b)

Fig. 3 - Reduction of radiating areas by means of twisted wires (a) in the toroidal inductor and (b) in the tracks of the PCB.

too. As a consequence, also the amount of radiated noise which can couple with the circuit conductors, thus becoming conducted noise, will be minimized. This is the reason why, even if the major concern of this design is the minimization of conducted EM noise, it is important to reduce the efficiency of the radiating sources as much as possible. In order to do that, another important practical provision is to twist the wires in the toroidal inductor used in the converter power stage and, if possible, all the critical tracks of the PCB, as shown in Fig. 3. This keeps the emitting areas as small as possible (introducing also a mutual cancellation of the fluxes), without compelling to excessively shrink the magnetics and the size of the printed circuit board (PCB), which is normally difficult and sometimes impossible.

All of these considerations have a quite relevant effect on the design of the PCB of the converter. As is shown in the upper part of Fig. 4, which represents the solder layer of the PCB, the tracks between the high frequency by-pass capacitors and the switching components are kept as short as possible and twisted according to what has been discussed so far. Moreover, this provision allows to increase the frequency of the resonance between the capacitors and the track stray inductance as much as possible. This helps to extend the effectiveness of the capacitive filter to higher frequencies.

Observing the PCB layout given by Fig. 4 it is possible to see that the track connected to the power switch drain, which exhibits very fast voltage variations during the switch commutations, is kept very short and shielded by means of two constant voltage tracks ($+V_{out}$ and $-V_{out}$) on the solder layer and a ground plane on the component layer, so as to minimize the generation of radiated EMI.

Also the gate circuit, which exhibits an high peak current, must be accurately designed according to the previously discussed guidelines. As already mentioned, the key factor is the area embraced by the circuit which must be as small as possible. This is particularly critical when it comes to the insertion of a suitably designed snubber

circuit (typically an R-C snubber). The snubber is highly recommended mainly to slow down the Mosfet turn-off and thus to reduce the power diode recovery current. Moreover, any ringing in the gate circuit can be greatly amplified in the drain; therefore, the adoption of the snubber is advantageous also to damp such oscillations.

Finally, the control circuit must be effectively protected against the disturbances by reducing the length of the sensitive tracks as much as possible. This is particularly important for the analog inputs of the control implementing the feedback loops for the regulation of the output voltage and input current. The corresponding tracks must be short and shielded by means of tracks exhibiting a stable voltage level and a low impedance to ground. In the component layer of the converter's PCB, which is shown in the bottom part of Fig. 4, a shield plane connected to the reference voltage is implemented which extends under the

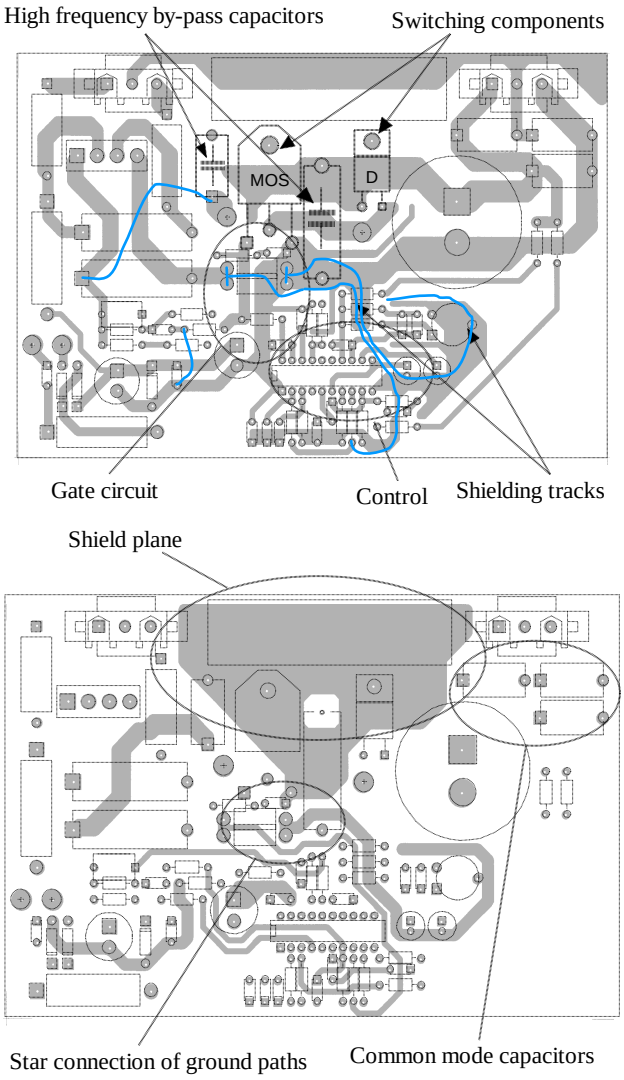

Fig. 4 - PCB of the converter: solder layer (top) and component layer (bottom). The size of the board is 150 mm x 100 mm.

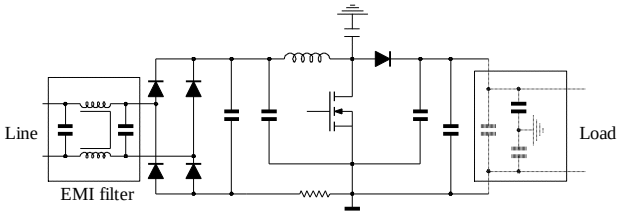

Fig. 5 - Schematic of the converter including input and output EMI filters.

power switching components and is connected to ground in a single point to avoid ground loops. It is important to notice the presence of common mode filter capacitors and of a single, star connection of the ground tracks, needed to avoid ground loops involving sensitive parts of the circuit (control circuit, gate circuit).

The design of the power stage can be completed by determining the common mode and differential mode input filters [15], depicted in Fig. 5, which represents the complete converter circuit. The input filter for the differential mode noise, which is a third order filter, can be designed calculating the maximum value of each harmonic component of the current ripple. The current ripple maximum amplitude is given by (1).

$$\Delta I_{max} = \frac{V_{out}}{8 f_s L} \cong 1.13A \qquad (1)$$

Assuming the ripple waveform to be triangular and varying the duty-cycle it is possible to find the maximum amplitudes of the harmonic ripple components which, of course, take place at different duty-cycle values. To perform the calculations it is assumed to have a 100Ω impedance towards the line, which is actually the equivalent differential mode impedance of the Line Impedance Stabilizing Network (LISN) requested by the standards. The results are reported in the third column of Table III. It is worth noting that the switching frequency has been selected so as to have the first and second harmonic component of the ripple below the lower frequency considered by the standards [4]-[5].

TABLE III
MAXIMUM EXPECTED VOLTAGE NOISE DERIVED FROM CURRENT RIPPLE HARMONIC COMPONENTS

1	*70 kHz*	*153 dB mV*	*87 dB mV*
2	*140 kHz*	*141 dB mV*	*57 dB mV*
3	210 kHz	134 dB µV	40 dB µV
4	280 kHz	128 dB µV	26 dB µV
5	350 kHz	127 dB µV	19 dB µV
6	420 kHz	125 dB µV	9 dB µV

Based on these calculated values, it is possible to determine the required filter attenuation and consequently the values of the differential mode inductors and of the

capacitors of the filter (Fig. 5). The required attenuation must be suitably oversized (at least 10 dBμV) to cope with the common mode component of the conducted noise and with possible resonances. Considering again the 100Ω load for the filter, it is then possible to calculate the expected filtered noise at the different harmonic frequencies. The resulting amplitudes are given in the fourth column of Table III. If the filter design is correct, these amplitudes must be well below the limits set by the standards. In this case, the values of the adopted inductive filters are L_{dm} = 70μH and L_{cm} = 6.8mH for the differential mode and common mode component respectively. The value of the line side filter capacitor is 1μF, while that of the rectifier side capacitor is 2μF. It is worth noting that, as shown in Fig. 5, a common mode capacitive filter is connected to the output of the converter, that is as close as possible to the major source of common mode noise.

Another important factor in reducing the generation of EMI in a switching converter is the modulation of the switching frequency. In developing the prototype, the shifting of the switching frequency has been simply implemented by adding to the ramp generator circuit of the controller a disturbance derived from the rectified input voltage. In this way the modulation frequency is no longer fixed, but is modulated at 100Hz around its nominal value (70kHz). It is worth noting that the disturbance signal is added to the ramp generator so as to get the minimum switching frequency when the commutated current is maximum.

IV. Experimental Tests on the Prototype

The converter prototype has been extensively tested to reveal potential sources of EMI and to test possible solutions before the final measurements have been done. As expected, the low frequency behavior of the PFC is very good, as can be seen in Fig. 6, where the good proportionality between line current and voltage can be appreciated. Fig. 7 describes the effect of the snubber adopted for the gate circuit. As can be seen, the insertion of the snubber reduces the speed of the commutation and the v_{GS} voltage ringing at turn-on (note that the time base is different for the upper and lower part of Fig. 7). Indeed, the v_{GS} voltage peak corresponding to the conduction of power diode recovery current summed to the inductor current, which is clearly visible in the upper part of the figure, is almost totally removed in the bottom figure, where the voltage sets to the level corresponding to the inductor current without appreciable ringing. This, as will be shown in the following, strongly improves the high frequency behavior of the converter.

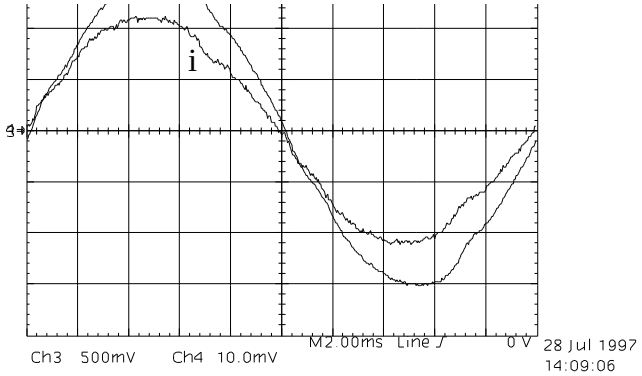

Fig. 6 - Line voltage (100V/div.) and current (2A/div.). Horizontal scale: 2ms/div.

The effect of the previously described switching frequency modulation is shown in Fig. 8, where the v_{DS} voltage spectrum is depicted. As can be seen, the effect of the switching frequency modulation is to modify the structure of the signal's spectrum. As expected, the spectrum is no longer composed by definite lines located at the multiples of the switching frequency, but is made up of large and flat bands, the biggest centered around the nominal switching frequency. The harmonics of the

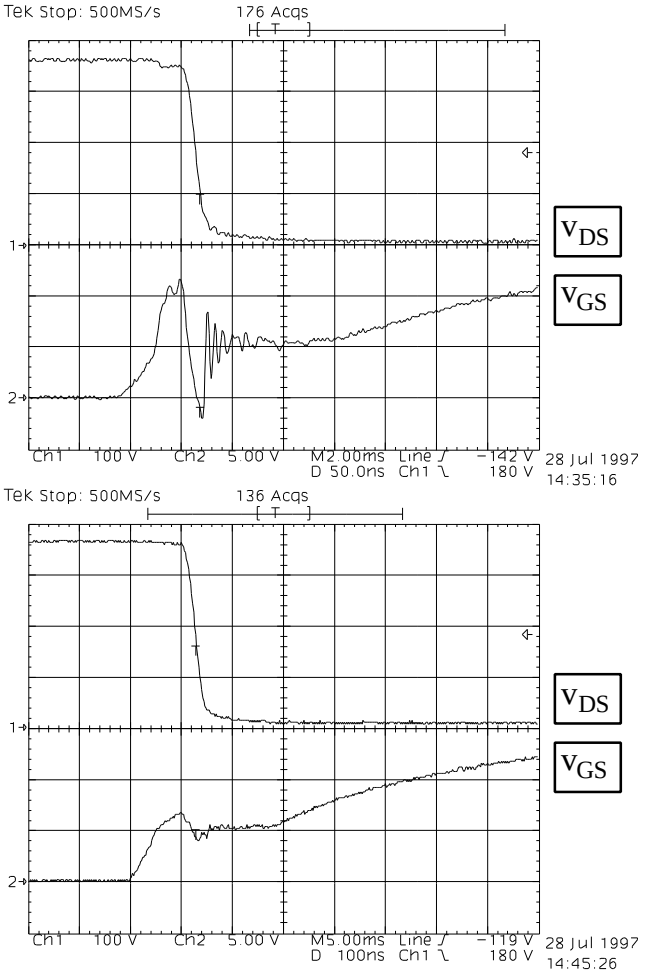

Fig. 7 - Gate circuit snubber effect at turn-on. Top: turn on without snubber. Bottom: turn on with R-C snubber. Note that the time base in the bottom figure is twice the preceding one.

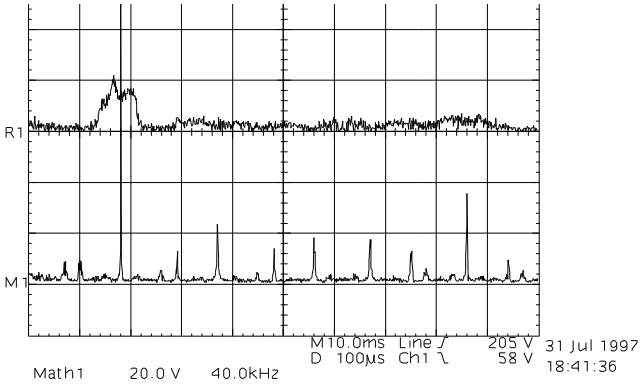

Fig. 8 - Switching frequency modulation effect on v_{DS} voltage spectrum. Upper trace: modulation on. Lower trace: modulation off.

switching frequency are, indeed, almost totally eliminated. This turns out in a very relevant improvement of the high frequency behavior of the converter, as will be shown in the following.

V. EMI Measurements

The developed Boost PFC, as schematically depicted in Fig. 5, has been tested according to the requirements of the EMC standards, which regulate the conducted EMI levels for this kind of electronic devices [4]-[8]. As required, the

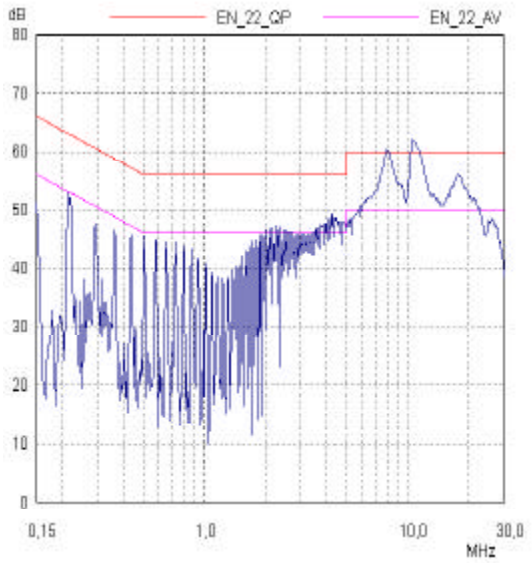

Fig. 9 - Conducted noise for the Boost PFC (peak measurement).

converter has been connected to a stabilized voltage source through a Line Impedance Stabilizing Network (LISN) and spectra of the input current have been measured in the range from 150kHz to 30MHz under different conditions. The result of the first test on the converter is shown in Fig. 9. As can be seen, while the converter's behavior at low frequencies is pretty good, there is an excessive high frequency content in the current spectrum. As can be noted, the low frequency part (up to 1MHz) of the noise spectrum is made of multiples of the switching frequency and is mainly differential mode noise. Its amplitude decreases with frequency thanks to the adopted differential mode filter. The high frequency noise is instead, mainly common mode noise.

Adding a common mode capacitive filter at the converter's input does not improve the situation as expected, because, as Fig. 10 shows, the differential noise increases due to the circuit unsimmetry determined by the asymmetrical location of the Boost inductor. This turns the increased common mode current into a differential mode current, thus worsening the low frequency performance of the converter. Moreover, the high frequency behavior is modified by the resonance between the common mode capacitors at the converter input and output and stray inductance of their connections.

To further confirm this interpretation of the measurements, the additional common mode filter is moved to the converter's output, in parallel with the one already located there. This determines a better low frequency behavior, since common mode currents can now circulate without affecting the LISN, but also a further worsening of the high frequency part of the spectrum because of the resonances of the newly inserted filter with the one already present on board and with the stray inductances of the connections, as is shown in Fig. 11. This implies that it is not always recommendable to put more capacitive filters in parallel, as is often done in practice, unless it is possible to keep the length of the connections very short and avoid the resonances, which strongly limit the effectiveness of the resulting combined filter.

To improve the system's performance at high frequency, a shield connected to the Mosfet source terminal is inserted between the switch and the heatsink. As Fig. 12 shows, this provision reduces the common mode noise and considerably improves both the low and the high frequency behavior of the converter because the capacitive currents coupled to the drain can now directly flow through the source without affecting the LISN. The shielding action introduced by this solution allows to reduce also the high frequency noise, but it is necessary that the connection of the shield is done very close to the source terminal of the Mosfet. An alternative solution is tested in Fig. 13, where the connection of the heatsink to the negative rail is considered. The heatsink acts again like a shield for the whole circuit, considerably reducing the noise level in the low frequency range. Because of the length of the connection, the effectiveness of this shielding action partially worsens in the high frequency range. A clear drawback of this provision is that the heatsink is no longer galvanically isolated from the circuit.

To verify the effect of the R-C snubber adopted for the gate circuit of the power Mosfet a spectrum measurement is performed disconnecting it from the gate, while

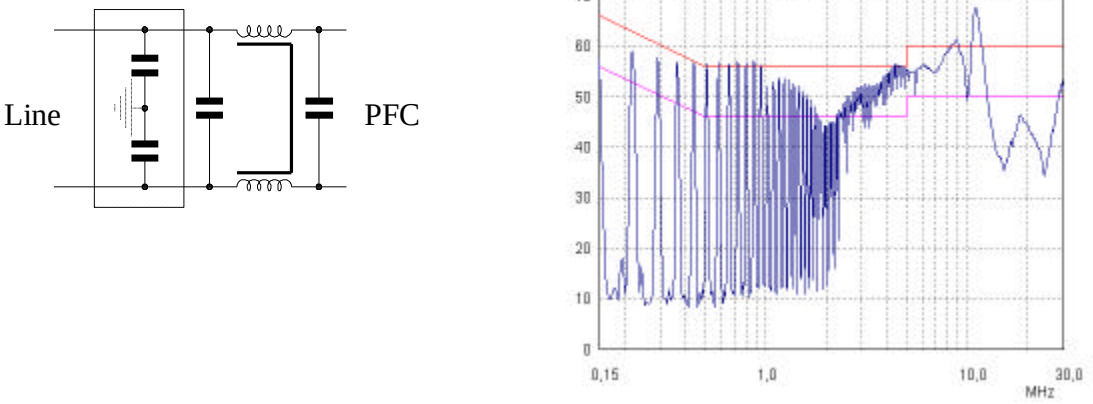

Fig. 10 - Effects of additional common mode capacitive input filter insertion (peak measurement).

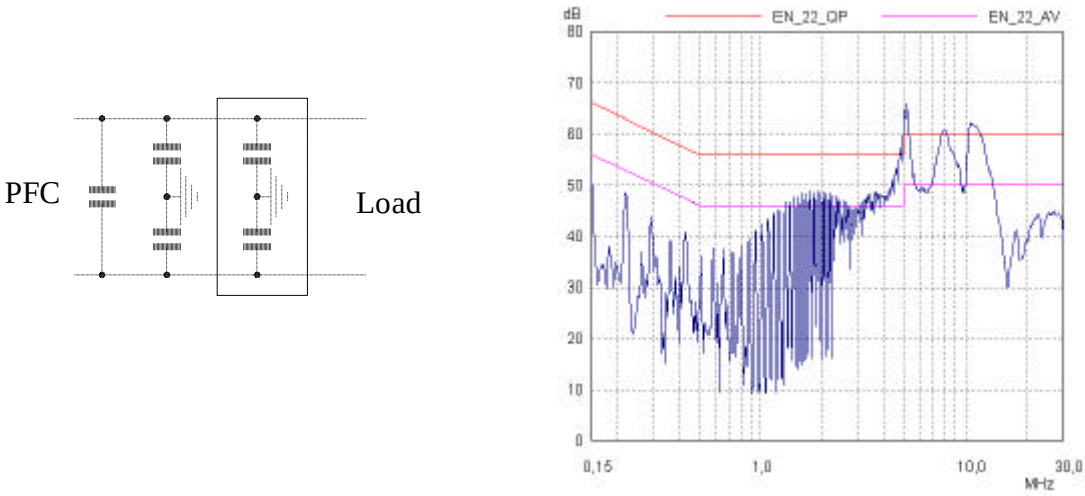

Fig. 11 - Effects of additional common mode capacitive output filter insertion (peak measurement).

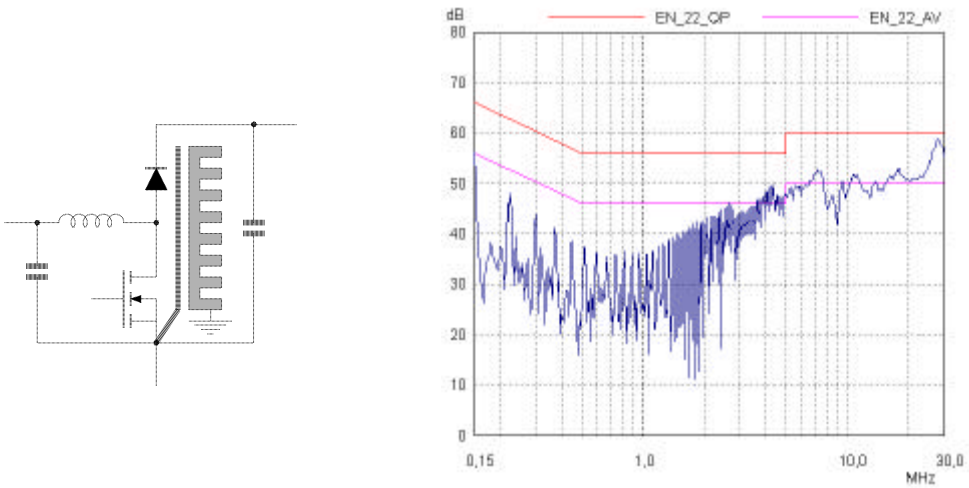

Fig. 12 - Effects of shield insertion between Mosfet and heatsink. The shield is connected to the Mosfet source (peak measurement).

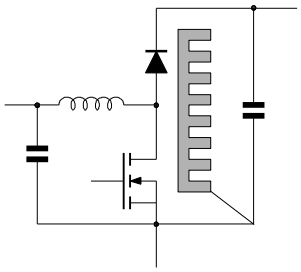

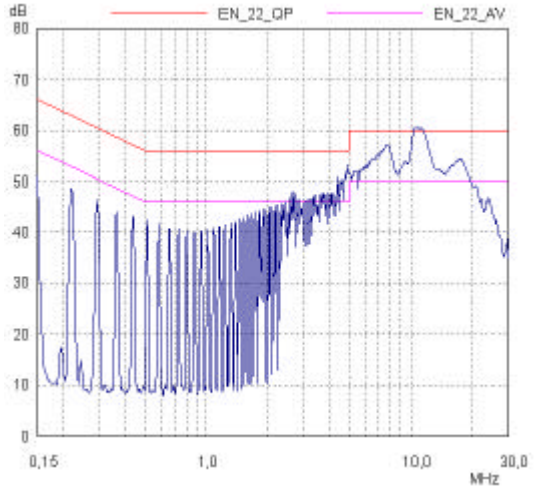

Fig. 13 - Effects of heatsink connection to the negative voltage rail not close to the Mosfet source (peak measurement).

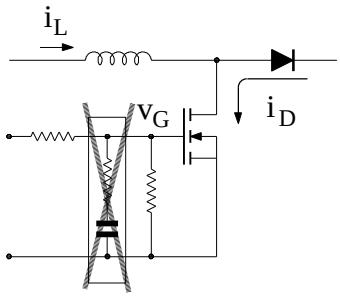

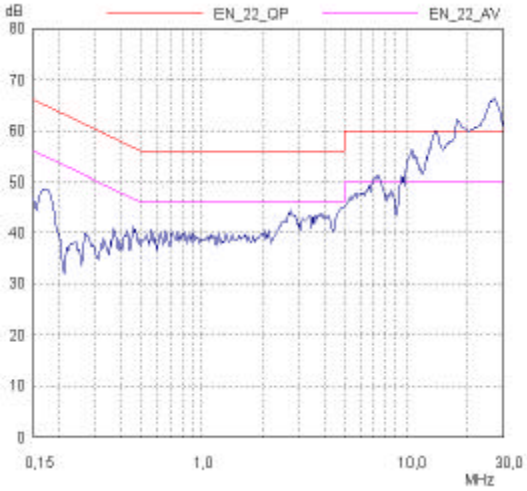

Fig. 14 - Effects of gate snubber disconnection (diode reverse recovery occurs) with switching frequency modulation (peak measurement).

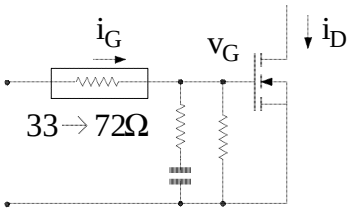

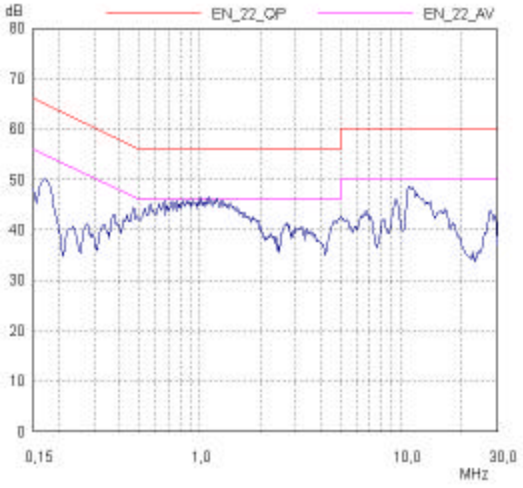

Fig. 15 - Effects of gate series resistance increase with switching frequency modulation (peak measurement).

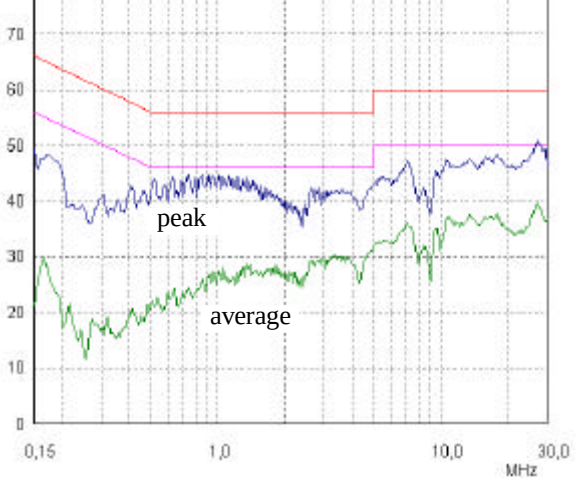

Fig. 16 - Final peak and average conducted noise measurements.

adopting the frequency modulation technique which was previously described. As is shown in Fig. 14, the snubber disconnection determines a considerable worsening of the high frequency part of the spectrum, which is due to the steeper transition of the v_{DS} voltage, which takes place at the snubber disconnection, and to the diode recovery current peak in the switch. To confirm this, the series gate resistor has been increased, further reducing the speed of the Mosfet commutations. As shown by Fig. 15, the high frequency part of the spectrum is improved as expected, while the low frequency behavior of the converter is almost unchanged.

Finally, the combined action of the switching frequency modulation technique and the gate snubber circuit is shown by Fig. 16. This reports both the peak and the average measured conducted noise and represents the final set-up measurements for the converter, including all the solutions which have been discussed throughout the paper. As can be seen, the low frequency part of the spectrum is greatly improved by the adoption of the switching frequency modulation, especially in the average noise measurement. In conclusion, Fig. 16 shows how the adopted solutions allow to achieve the full compliance of the converter conducted emission with the considered standards.

VII. Conclusions

The paper presents the development of a 600W Boost PFC compliant with the high frequency conducted EMI limits set by EN50081 standards. Different design options are considered and experimentally tested. The effectiveness of some particular provisions, such as the snubber gate circuit or the modulation of the switching frequency, in reducing the conducted noise, is clearly demonstrated by a complete set of EMI measurements.

References

[1] IEC 1000-3-2: 1995 “Electromagnetic compatibility. Part 3: Limits - Sect. 2: Limits for harmonic current emission (equipment input current ≤ 16A per phase)”.

[2] IEC 1000-4-1: 1992 “Electromagnetic compatibility. Part 4: Testing and measurement techniques. - Sect. 1: Overview of immunity tests. Basic EMC publication”.

[3] IEC 1000-4-7: 1991 “Electromagnetic compatibility. Part 4: Testing and measurement techniques. - Sect. 7: General guide on harmonics and interharmonics measurements and instrumentation, for power supply systems and equipment connected thereto”.

[4] EN 50081-1: 1992 “Electromagnetic compatibility - Generic emission standard. Part 1: Residential, commercial and light industry”.

[5] EN 50081-2: 1993 “Electromagnetic compatibility - Generic emission standard. Part 2: : Industrial environment”.

[6] EN 50082-1: 1996 “Electromagnetic compatibility - Generic immunity standard. Part 1: : Residential, commercial and light industry”.

[7] EN 50082-2: 1995: “Electromagnetic compatibility - Generic immunity standard. Part 2: : Industrial environment”.

[8] CISPR 16: 1993 “Specification for radio disturbance and immunity measuring apparatus and methods”.

[9] L.Rossetto, A.Zuccato: Tutorial on "Understanding and complying with CISPR and IEC 1000 standards on EMC", European Power Electronics and Drives Conference, Trondheim (Norway), 1997.

[10] R.Redl: Tutorial on "Low-cost line harmonics reduction", IEEE Applied Power Electronics Conference, Dallas, 1995.

[11] P.Tenti, G.Spiazzi: Tutorial on "Harmonic limiting standards and power factor correction techniques". European Power Electronics and Drives Conference, Sevilla (Spain), 1995.

[12] L.Rossetto, G.Spiazzi and P.Tenti: "Control techniques for power factor correction converters". International Conference on Power Electronics and Motion Control, Warsaw, Sept. 1994, pp.1310-1318.

[13] R.Redl, P.Tenti, J.D.van Wyk: "Combatting the pollution of the power distribution systems by electronic equipment". IEEE Applied Power Electronics Conference, Atlanta, Febr. 1977, pp.42-48.

[14] Clayton R.Paul: "Introduction to Electromagnetic Compatibility". John Wiley &Sons, Inc. 1992.

[15] R.L.Ozenbaugh: “EMI filter design”. Marcel Dekker Inc. New York. 1996.

[16] D.A.Weston: “Electromagnetic Compatibility. Principles and applications”. Marcel Dekker Inc. New York. 1991.

[17] R.Redl: Tutorial on "Fundamentals of electromagnetic compatibility in power electronics". IEEE Applied Power Electronics Conference, San Jose, 1996.

[18] G.Goldberg: "Low-frequency and high-frequency EMC in power systems", International Symposium on EMC, Zurich, March 1991, paper Q-118.